Investigating the Influence of Length and Cross Sectional Area in Heat Storage Thermal Stratification

Amos Veremachi & B.C.Cuamba
Department of Physics
Eduardo Mondlane University
Maputo, Mozambique
averemachi@gmail.com

Ole J.Nydal & J.Lovseth
Department of Energy and Process Engineering
NTNU
Trondheim-Norway
Azhar Zia
Department of Physics
Uppsala University-Sweden

Abstract- In order to overcome the limitations imposed by the intermittent nature of solar radiation on its different applications, energy storage is an important component of any solar system. More specifically, the incorporation of thermal energy storage makes it possible to store the collected solar thermal energy and use it during off-sun periods, for multiple domestic needs (e.g. cooking, heating, etc). For this to happen, heat must be extracted from the storage to the utility. In order for the extraction process to be done in an efficient way, thermal stratification of heat storage is beneficial. Through comparison of hourly temperature profiles of three different rock-bed heat storages, this paper discusses the influence of length and cross-sectional area of the storage on its thermal stratification. Preliminary findings suggest that by increasing length and reducing diameter of the storage, its thermal stratification is enhanced.

Key words: solar thermal energy, renewable, prototype, rock bed, heat storage, stratification, Temperature gradient.

I. INTRODUCTION

Mozambique share the same characteristic as many other African countries, in that the major part of the population lives dispersed in rural areas. Far from national electricity grid, this majority of population relies on biomass (firewood) as a major source of thermal energy for the satisfaction of their multiple domestic energetic needs. Currently, however, this source of energy is becoming scarcer due to several factors (e.g. unsustainable use of forest resources, land use for agricultural practice, desertification, etc) which forces people (in particular women and girls) to dedicate much of their time in walking long distances to fetch firewood at expenses of many other activities-including education. Nevertheless, the high intensity of different renewable sources of energy in this country, in particular solar energy, opens some windows of solutions through small scale solar energy technologies which make solar energy a potential source of energy to be harnessed and used for different purposes, including cooking.

In fact, the gains of the adoption of different solar cooking technologies are recognized in many studies. For instance women and girls may dedicate much of their time to educational activities, which clearly have a potential to bring more women empowerment in developing countries, improve the quality of life (as the in-door environment becomes less exposed to smoke generated by incomplete combustion of row firewood) and improve the quality of natural environment (as mitigation of deforestation is likely to occur).

More aware of these gains, some countries embraced solar cooking technologies (Nepal, Kenya, India, Uganda, etc) but the most widespread technologies enable for direct cooking. A thorough and updated review on the design, development, implementation, performance and comparative studies of different solar cookers is provided in [1] and also SCInet (Solar Cookers International Network) on the dissemination of solar cookers in different countries and continents.

Direct solar cookers (like panel solar cookers, solar box cookers and direct focusing solar cookers) despite their advantages, present some constraints. One of the limitations is related to the fact that the cooking process is possible only in the presence of solar radiation, and some of them require long time to complete the cooking process beside that the person performing the cooking is subjected to face the sun rays [1] which might pose some health risks due to excessive exposure to solar radiation. These limitations may be overcome by adopting indirect solar cooking techniques, which bring into the scenario the thermal storage system.

Storage of solar thermal energy brings more flexibility to the utilization of thermal energy generated from solar systems and increases their reliability. In fact through thermal energy storage, solar thermal energy become available when is needed and energy output can be adjusted to load demand [2]-[3]-[5]; in addition heat storage (HS) improve performance of solar systems and play a paramount role in energy conservation; thus turning the field of solar energy more competitive, cost effective by reducing associated costs [4]-[5].

The three main design criteria of a solar thermal energy storage system should be based on excellent technical properties, cost effectiveness and low environmental impact of the storage materials [6].

Within the category of technical properties, three aspects are emphasized: a high thermal storage capacity which leads to reduction of system´s volume (hence reduced costs for insulation) and increased efficiency, good heat transfer rate

between the storage material and the heat transfer fluid (HTF) which enable the release and absorption of heat as fast as required; and good stability in order to prevent chemical and mechanical degradation after several thermal cycles.

A. Types of Thermal Storage Systems

Thermal energy can be stored in different medium as sensible heat, when it involves change in internal energy of the material by raising its temperature. The amount of energy stored in a material as sensible heat is a function of the amount of storage material, of its specific heat capacity and of the temperature change experienced by the material, when its temperature is raised from some initial value T_1 to a final value T_2.

$$\delta Q = m \times c_P \times dT \Rightarrow Q = \int_{T_1}^{T_2} m \times c_P \times dT = \int_{T_1}^{T_2} V \times \rho \times c_P \times dT \quad (1)$$

In the above expression, ρ is a density of material, V its volume and c_P the material´s specific heat capacity.

It can also be stored as a latent heat -when the storage material undergoes phase change at constant temperature (temperature of phase transition). If the temperature of a substance, with phase change temperature T_{ph}, is raised from T_1 to T_2 such that $T_1 < T_{ph} < T_2$, the amount of energy stored by a material of mass m and specific heat capacity c_P is given by the expression:

$$Q = \int_{T_1}^{T_{ph}} m \times c_{P,1} \times dT + m \times L + \int_{T_{ph}}^{T_2} m \times c_{P,2} \times dT \quad (2)$$

Here $c_{P,1}$ and $c_{P,2}$ are specific heat capacity at constant pressure of the material at the initial phase and the phase after the transition, respectively; L is a heat of phase transformation.

Energy can also be stored as thermochemical energy when internal energy of the material is changed as a consequence of energy absorbed in breaking or reconfiguring molecular bonds in a reversible fashion.

$A + \Delta H \rightarrow B + C$ Forward reaction (ΔH is the endothermic heat of reaction) (3.a)

At elevated temperatures the backward reaction takes place during which the original chemical system is formed while at the same time energy is released.

$$B + C \rightarrow A + \Delta H \quad (3.b)$$

The quantity of energy stored depends on the heat of endothermic reaction, the quantity of the storage material and the extent of reaction:

$$Q = f_r \times m \times \Delta H \quad (4)$$

Where f_r, is the fraction of material reacted.

Therefore, thermal energy storages can be grouped into three general categories, namely sensible heat storage, latent heat storage and thermochemical heat storage [3]-[4].

Integrated within a context of a Network project supported by NUFU program-Norway, this study embraced the challenge of developing a prototype of a small scale solar energy concentrating system with heat storage, that would enable the collection of solar thermal energy and its storage for later use during off sun periods (night or cloudy days) for multipurpose domestic needs satisfaction. However, for the heat extraction from the storage to appliances to be done in an efficient way, good and stable stratification is important.

Early storage prototype using atmospheric air as heat transfer fluid and rocks as heat storage medium have been numerically and experimentally studied, see [1]-[2].

Experimental results reported in [1] reveal that after charging the wider and shorter storage prototype, temperature equalization within different sections of the storage was a dominant phenomenon upon after.

In this study, the influence of length and cross sectional area of the rock bed heat storage on its thermal stratification is experimentally investigated.

II. Theory and The Governing Equations:

The packed bed can be regarded as a system that comprises a solid storage material and HTF that is circulated through the voids in HS in a process involving forced convection.

The fluid enters the storage at high temperature and as it goes through the voids it gives up heat to the rocks and emerges at the exit at low temperature. As a consequence the bed temperature rises. In this process, some of the important characteristics are heat transfer and pressure drop in the HS. In which case some of the recommended equations are:

$$\Delta p = \frac{L \times G_o^2}{\rho_{air} \times D} \times \left(21 + 1750 \times \frac{\mu}{G_o \times D} \right) \quad (5)$$

$$h_v = 650 \times \left(\frac{G_o}{D} \right)^{0.7} \quad (6)$$

Where D and G_o are average particle diameter and mass velocity, respectively; and are given by:

$$D = \left[\frac{6 \times V_o \times (1 - \varepsilon)}{N \times \pi} \right]^{\frac{1}{3}} \quad (7)$$

$$G_o = \rho_{air} \times v_{air} \quad (8)$$

In these equations N is the number of pebbles in a vessel of a volume V_o. Pebbles are assumed to be of a spherical form, ε is a void fraction; ρ_{air} and v_{air} are air density and velocity respectively; L and μ are bed length and kinematic viscosity of air, respectively.

Given that the storage diameter is smaller, a 1-D unsteady energy conservation formulation is more appropriate to describe the heat transfer phenomenon (Schumann model) [7]. In this line of thoughts, the governing differential equations

for the fluid and solid phase temperatures are, respectively given by:

$$\left(\rho c_P\right)_f \times \varepsilon \times \frac{\partial T_f}{\partial t} = -\frac{\left(\dot{m} c_P\right)_f}{A} \times \frac{\partial T_f}{\partial y} + h_v \times \left(T_s - T_f\right)$$

(9)

$$\left(\rho c_P\right)_s \times \left(1-\varepsilon\right) \times \frac{\partial T_s}{\partial t} = h_v \times \left(T_f - T_s\right)$$

(10)

The symbols T_f and T_s refer to fluid and storage (or rock) temperature respectively, h_v is the volumetric heat transfer coefficient and the indexes f and s refer to fluid and storage, respectively.

The use of air as HTF in high temperature HS is challenging. To be more effective the system must be air tight (with no leakages). Besides normal heat losses through insulation to ambient due to temperature difference, the presence of elbows in some of the HS leads to additional losses potentially due to leakages. An attempt was made to use glue in order to ensure the system was air tight, but this was proven to be not feasible at temperatures above 300 °C because the glue could not withstand those temperatures, leading to potential leakages at the connections. Therefore, one of the assumptions behind Schumann model, namely that related to negligibility of heat losses to ambient may not appropriate in this setup. The accountability of heat losses to the surrounding environment brings an additional term in the equations above:

$$\left(\rho c_p\right)_s \times \left(1-\varepsilon\right) \times \frac{\partial T_S}{\partial t} = h_v \times \left(T_f - T_S\right) + A_{TS} \times U_{ov} \times \left(T_{sav} - T_a\right)$$

(11)

The symbols A_{Ts}, U_{ov}, T_{sav} and T_a stand for total storage area, overall heat transfer coefficient, average storage temperature and ambient temperature, respectively.

During charging, air comes from the outlet at mass flow rate $\dot{m}_{air}$ and initial temperature T_o, and then is heated to T_{inlet}. The power gain by air is given by:

$$\dot{Q} = \dot{m}_{air} \times \int_{T_o}^{T_{inlet}} c_{P_{air}}\left(T\right) \times dT \qquad (12)$$

The energy stored in the bed by the end of charging process is given by:

$$Q = \int_0^L m_s \times c_{Ps} \times \left(T_s\left(y\right) - T_{os}\right) dy \qquad (13)$$

Here t_{Total} stands for total duration of the charging process.

And the stratification parameter is given by:

$$\eta_{strat} = \frac{T_{\max} - T_{out}}{T_{\max} - T_{\min}} \qquad (14)$$

B. Heat losses:

When it comes to high temperature HS systems, finding appropriate insulation to minimize heat losses to ambient becomes one of the major challenges. As such the estimation of heat losses to ambient is one of common practices. Heat losses from insulated systems to ambient can be estimated by the following expression:

$$\dot{Q}_{loss} = U \times A \times \left(T_{av} - T_{amb}\right) \qquad (15)$$

Where $U = \dfrac{1}{\dfrac{1}{\alpha_{out}} + \dfrac{\delta_{wall}}{k_{wall}} + \dfrac{\delta_{insul}}{k_{insul}} + \dfrac{1}{\alpha_{in}}}$ is the overall heat loss coefficient from system to the surroundings and A is the total surface area of the HS. In the present paper a simplified method will be adopted, in which case the HS system is wrapped up with N layers of different types of insulation and

$$U = \frac{1}{\sum_{j=1}^{N} \dfrac{\delta_{jinsul}}{k_{jinsul}}} \qquad (16)$$

In formulae above α represents heat transfer coefficient of a surface, δ represents thickness and k thermal conductivity of material.

In $[2]$ simulation results revealed 0.5 m thicker Rockwool with 5 layers of reflective Al-foils evenly spaced and inserted in between could lead $U = 0.075\ \dfrac{W}{m^2 K}$. An effective heat loss reduction by a factor of two seems to be achievable by space evacuation or use of reflecting shields; but the most dramatic heat loss reduction is attained by combining space evacuation and reflecting shields which has a potential to reduce heat losses in more than a factor of 20 as reported in $[10]$. In the set up under consideration rockwool was used as insulation material.

METHODOLOGY

To evaluate the influence of storage length in the heat storage's thermal stratification, two rock bed heat storages of different length but same cross sectional area were built out of pipes with 160 mm diameter and used for in-door testing in the Lab of Department of Energy and Process Engineering-NTNU. The long rock-bed heat storage (HS) is 3.4 m length, the shorter storage is 1.56 m length. Both were filled with pebble stones (void fraction 0.38) and insulated from the environment using two layers of rock wool thermal insulation (each layer 50 mm thick). While the long rock-bed HS was filled with 114 kg of pebbles, the smaller rock-bed was filled with 49.5 kg of the same rock sample. Rock samples were completely washed. In Table.1 properties of the used rock sample are presented.

Parameter	Value	Unit
Equivalent diameter	0.04	m
Density of rocks*	2630	Kg/m^3
Specific heat capacity*	830	J/kg°C
Thermal conductivity*	2.79	W/m.K
Void fraction	0.38	
(ρc_P)	2.183	MJ/m^3K
Average particle diameter	0.028	m

*Adopted from [1].

Fig.1.This picture shows river gravel samples (pebbles) used in the experiments under consideration.

Both HS were insulated and in the following sentence properties of insulation are presented.

The long rock bed HS was insulated by 2 layers of insulation, each 5 cm thicker. The first layer was made by Glava insulation, density $40\,\frac{kg}{m^3}$ and thermal conductivity presented in fig.2. The second layer was made by FyreWrap Blanket Insulation, density $96\,\frac{kg}{m^3}$, R value of $1.46\,\frac{m^2K}{W}$ and thermal conductivity presented in figs 2 and 3.

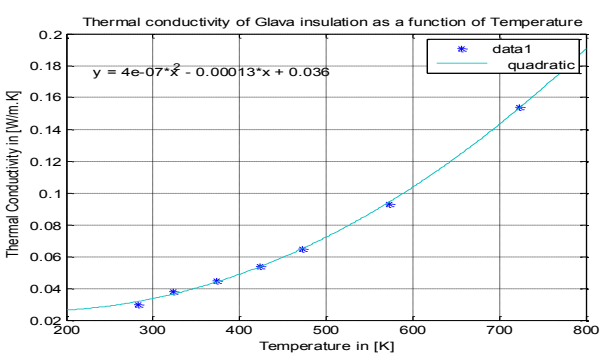

Fig.2.This chart shows thermal conductivity of Glava insulation as a function of temperature. Data from the manufacturer.

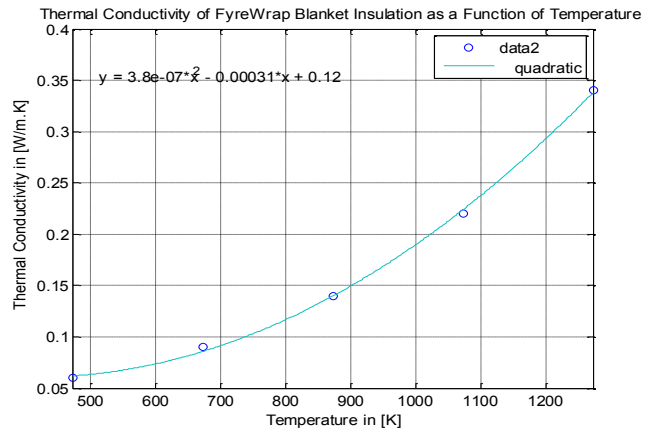

Fig.3.This chart shows temperature dependence of thermal Conductivity of FyreWrap Blanket Insulation. Data from manufacturer.

During the experiments both storages were charged using hot air at different but constants flow rates and inlet temperatures. A hose provided a connection between the compressed air outlet and an electric heater, which in turn was connected to the storages' inlet.

For logging temperatures of the storage in different sections, 16 thermocouples were used for the 3.40 meter heat storage and 11 for the 1.56 meter storage and connected to a data logger which in turn was interfaced to a PC hosting a labview program.

For the long HS, thermocouples sensing the temperature at the inlet and at the outlet were placed 5 cm from the openings, while the others were 20 cm apart from each other.

Temperatures in different sections of the heat storage were recorded in both charging and discharging modes in 1 second time intervals.

Techfluid flowmeter series EC 250 was used to measure the air flow rates at ambient temperature, while the valve at the outlet of compressed air system was used to regulate and adjust the flow rate at the desired level.

In order to access the influence of length in the thermal stratification of the storage, the temperature profiles of the two HS, charged at the same mass flow rates, were compared.

To determine the influence of the cross sectional area of the storage on the thermal stratification the results of the two storages were compared with early results from experiments performed by Okello using a more wider but short storage. The dimensions were 400 mm diameter and 900 mm length. Pebbles were also used as storage material in the set up.

Pressure drop was measured for different air mass flow rates at the storage feeding point using a digital barometer VelocCalc TSI Plus, Model 8388-M-GB. The measurements were taken in three different points along bed diameter and then averaged for each mass flow rate. It is known that pressure drop determines the power requirements to charge or discharge the rock-bed.

Fig.4.This picture shows the long rock-bed HS to which electric air heater is connected.

The void fraction was estimated by first completely filling a bucket of known volume with pebbles, then by using a graduated bicker pouring water into the bucket until the level of rocks is reached. The ratio between the volume of water poured in and the volume of the bucket gives the void fraction. This is equivalent to the expression:

$$\varepsilon = \frac{V_b - V_s}{V_b} \tag{13}$$

Here V_b and V_s refer to volume of bucket and bulk volume of rocks in the bucket, respectively.

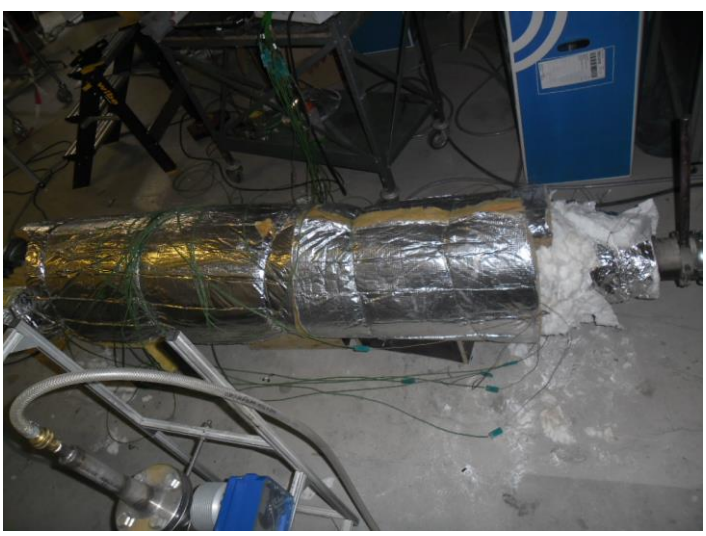

Fig.5.This picture shows the small rock-bed HS.

To estimate heat loss from the HS to ambient, the rock-bed was charged to a certain temperature and then left to go through degradation process in which case both the feeding port and the air exit port of the storage were covered with insulation and left for several hours while recording temperatures in different sections.

The maximum energy that can be stored in rock-bed heat storage can be calculated by the expression:

$$Q_{St} = m_s \times c_{P_s} \times \left(T_{\max} - T_{\min}\right) \tag{14}$$

Where m_s and c_{P_s} are mass of storage material and its specific heat capacity, respectively.

In the setup under consideration this heat is transmitted by hot air, therefore following $[6]$ the energy to be stored can be given by the formula:

$$\dot{Q} = \dot{m}_f \times c_{P_f} \times \left(T_{\max} - T_{\min}\right) \tag{15}$$

Here $\dot{m}_f$ and c_{P_f} is the mass flow rate and specific heat of HTF, respectively.

During charging process different rock-bed sections are at different temperatures each time the HS temperature profile is evaluated. Therefore rough estimates of the energy stored at the end of a certain time interval may be obtained by averaging temperatures of different bed sections and calculate its variation from the temperature of the HS when the charging process was started. Hence the expression given in [1] seems reasonable:

$$Q_{St} = m_s \times c_{P_s} \times \left(T_{\max_{av}} - T_{\min_{av}}\right) \tag{16}$$

Here $m_s = \rho_s \times V_T \times \left(1 - \varepsilon\right)$ (17)

Where V_T is the total volume of the storage.

Due to heat losses to the surroundings the stored energy will eventually decrease over time and by plotting the stored energy as a function of time duration of degradation process the estimate of the rate of heat loss to the surrounding as a function of time is enabled. In fact the rate of heat loss may be regarded as a slope of the graph of stored energy versus storage time, more details in [1].

III. Results and Discussion

For the long rock-bed, it was observed that high amount of time is required for the thermocouples located far from the storage feeding point to register high temperatures. This phenomenon was observed for different mass flow rates used to charge the storage. For the small HS, however, less time is required to charge the storage and thus for the heat front to travel along the rock-bed.

As can be seen from comparison between charts on figures 6 and 7 both long and short storages were charged nearly at same temperature of 330 °C and same mass flow rates of 2.4 g/s; while the long rock-bed HS required 9 hours to attain a temperature of 50 °C at the exit port, the shorter rock-bed required only 2.5 hours (just above $\frac{1}{4}$ of that time) to achieve the same temperature at the air exit port.

At this mass flow rate, and geometric characteristics of the bed and rock properties, the volumetric heat transfer coefficient was found to be around $3532.0\ W/m^3K$.

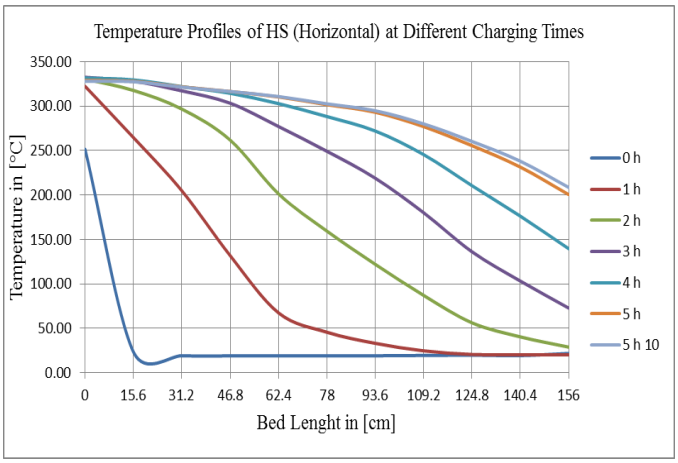

Fig.6. Shows temperature Profiles of a Rock-bed HS for different Charging times, at mass Flow rate of 2.4 g/s.

From the same charts it can also be seen that by the end of 5th hour of charging at both storages, while by then the air leaving the long storage outlet was at ambient temperature, at that time on the shorter storage heat was expelled to the surroundings at temperature of 200 °C.

The observed phenomenon suggests that for two storages charged at the same mass flow rate, the difference between the temperatures of hotter part of the storage and cooler part of the storage increases with increasing the length of the storage and decrease when the length is reduced. More specifically, **temperature gradient increase with increasing length**. This means that it take less time for the shorter HS to rise the temperature of the air leaving the storage, thereby starting pumping heat to the ambient than it takes for the long HS. This result is similar to that reported in [8]. In fact, as recognized in [12] having a sharp temperature front progressing along the bed is the best way to store and extract thermal energy.

The fact that the two HS, in comparison, have the same cross-sectional area and different lengths imply that their volumes are also different, hence they host different amount of storage materials. While the long HS presents a linear density of $33.53\ \frac{kg}{m}$, the smaller HS presents $31.73\ \frac{kg}{m}$ which is slightly lower and corresponding to 94.63 % of that presented by long HS.

Resulting from this difference their heat capacity is also different. In fact it would require more heat to rise the temperature of the long HS in 1 °C than is required in smaller HS.

At the end of five hours of charging the stratification parameter for the smaller rock-bed HS was 42 %; while for the same time interval the stratification parameter for the long rock-bed HS was 99.69 %. After 11 hours of charging the stratification parameter for the long rock-bed was 78.34 %. This fact suggests that stratification is enhanced by increasing the bed length.

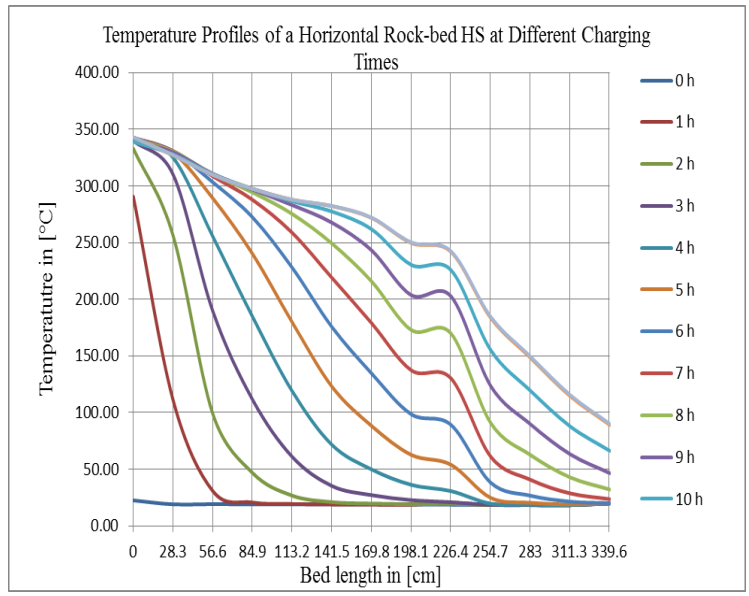

Fig.7. Shows temperature Profiles of a Horizontal Rock-bed HS at Different Charging Times, charged at mass flow rate of 2.4 g/s.

Results from another experimental study reported in [1] show that a 900 mm rock-bed HS with a diameter of 400 mm using pebbles was continuously charged at mass flow rate of 2.4 g/s and inlet temperature of 330 °C. The results indicate that at the 6th hour of charging the air left the storage nearly at 48 °C. While preliminary results in this study showed that the long storage charged at the same mass flow rate of 2.4 g/s required almost 9 hours for the exiting air to achieve almost the same temperature, see fig.7.

It should be noted that the long storage in the present study has half of volume as compared to the storage used in [1] but using similar rock samples. In addition to this the storages under consideration have different lengths and cross-sectional areas, hence different volumes. As a consequence they hold different heat capacities due to difference on the amount of storage materials. In literature, both length and cross-sectional area are reported to have impact on rock-bed HS stratification, with cross-sectional area having the major impact than length [11]. Therefore, the observed phenomenon could be due to differences in cross-sectional area or difference in lengths. In fact, for the same volume any change in cross-sectional area would affect its length and vice-versa. Thus stratification is enhanced by minimizing cross-sectional area normal to the fluid flow direction and also by increasing the length of the storage. A parameter that could be used to evaluate the impact of both cross-sectional area and length of the storage is the ratio of radius of the storage to its length. In which case seems reasonable to say the less the ratio the more stratified the HS becomes.

Comparison of the performance of the smaller rock-bed HS with results from the 90 cm storage reported in [1] reveal that the smaller HS reported in this study charged at the same mass flow rate and inlet temperature was less stratified. The smaller rock-bed in this study has its length slightly high than that reported in reference [1] but at the same order of magnitude and different in their cross-sectional area. It was expected that this comparison would elicit the role of cross-sectional area in the storage's thermal stratification. In some studies reported elsewhere it is suggested that by reducing the cross sectional area, stratification is enhanced. Result from this study seems to suggest the existence of other factors at play that needs to be elicited. In fact the storage capacity is also an important factor.

In order to ensure the suitability of the designed thermal energy system to its intended applications, the rate of thermal decay must be known. In the context of the present study an attempt was made to estimate systems heat loss to ambient. The following chart shows thermal degradation of HS during the storage time.

As can be seen from the chart the temperature of the hotter part of the storage decreased by nearly 27.6 % of its initial temperature in 6 hours of storage time (from ≈ 348 °C to nearly ≈ 252 °C). By the end of 12 hours of storage the hotter part was still at useable temperature of 200 °C. While the cooler part of HS experienced minor but progressive decrease in temperature. This fact atest to the fact that the major driving force for heat trasnfer between two medium is the temperature difference between them. The bigger the temperature difference the high the rate of heat loss.

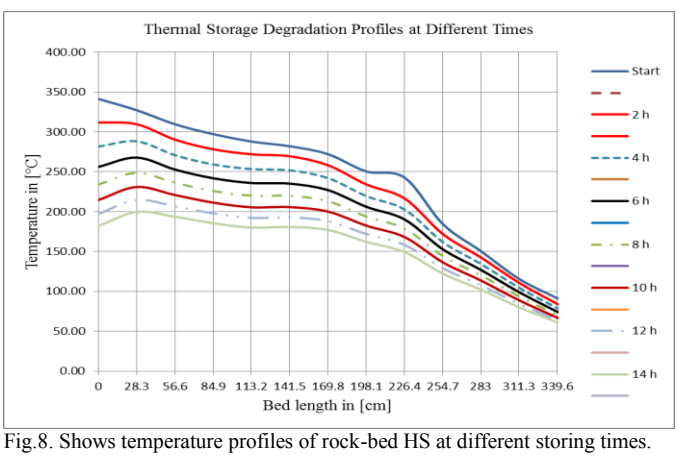

Fig.8. Shows temperature profiles of rock-bed HS at different storing times.

The chart in fig.9 shows the transient profile of the average stored energy in a rock-bed HS. As can be seen, the stored energy decreases with time and its behaviour is better described by a quadratic function. This decrease with time is due to heat losses to the ambient. In fact, starting with $Q_{st} = 21139054.2\ J$, after 7 hours of storage the stored energy decrease by 4262631 J ($\Delta Q_{st} = -4262631\ J$) corresponding to 20 % of stored energy lost to ambient.

It is interesting to note that from fig.10, the rate of heat loss to ambient decrease with stored time. This is understandable because as the storage get cooler the temperature difference with ambient decreases and with it the heat transfered to ambient also decrease.

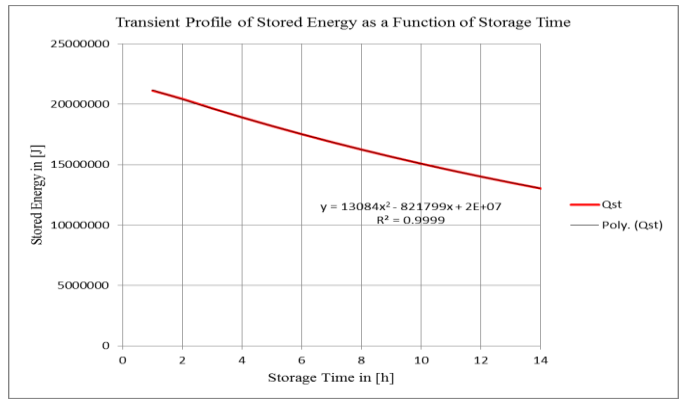

Fig.9. Shows average stored energy as a function of time.

From fig.10 it can be seen that the average heat loss rate decreases linearly with storage time. Initially, the average heat loss rate was around $\dot{Q} \approx 228.3\ W$; after 7 hours of storage time it went down to $\dot{Q} \approx 177.4\ W$ corresponding to nearly 22.3 % reduction. It should be noted that the overall insulation thickness used in the setup was 10 cm (2 layers). So, it is expected that by increasing more layers heat losses would witness a considerable reduction, thereby increasing time of useful energy availability in the HS.

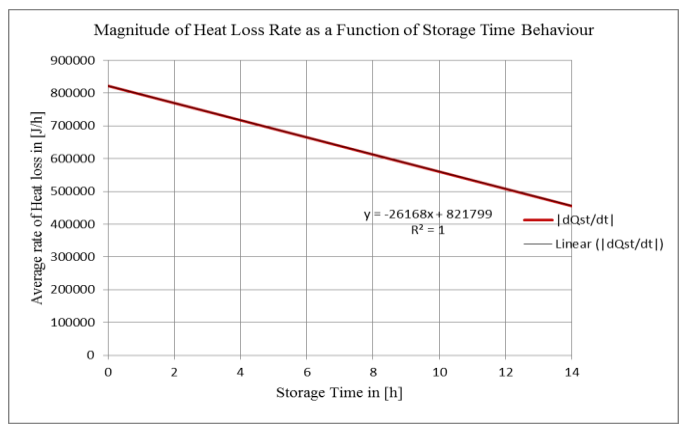

Fig.10. Shows average magnitude of heat loss rate as a function of storage time.

The storage was charged at different flow rates 2.4 g/s, 3.34 g/s and 4.8 g/s. The charging time was found to increase with decreasing flow rate, but pressure drop showed a positive correlation with mass flow rate. The correlation between pressure drop and mass flow rate was found by plotting the collected data in Matlab and the Matlab polyfit was used to generate the function.

$$\Delta p = 2.4\dot{m}^2 - 8.7\dot{m} + 11 \tag{18}$$

The power required to pump air through the HS, is given by

$$P = \frac{\dot{m}}{\rho} \times \Delta p \tag{19}$$

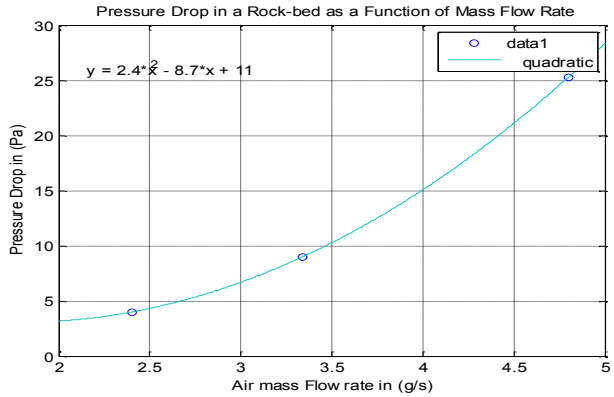

Fig.11. Shows pressure drop in a long HS as a function of mass flow rate.

IV. Conclusions and Recommendations

The influence of length and cross-sectional area on thermal stratification was experimentally investigated in this study by using indoor test results from three rock-bed heat storages that use air as HTF. The results show that increase in length leads to an enhanced thermal stratification. However further investigation is required in order to understand the role played by the cross-sectional area in stratification of the rock-bed in the prototypes in use. In order to ensure efficient storage, the system should be well insulated and air tight. Heat losses were observed to reduce over storage time attesting consistence with the fact that temperature difference between the system and ambient is a major driving force for heat transfer between the mediums.

By increasing insulation layers it should be possible to reduce heat losses to ambient to levels that may sustain thermal energy availability for the satisfaction of households needs.

References

[1] Okello, D. (2012). Rock Bed Stove Suitable for Solar Cookers With Thermal Energy Heat Storage Systems. PhD Thesis. Makerere University-Uganda.

[2] Chikukwa, A. (2008). Modelling of a Solar Stove: Small Scale Concentrating System With Heat storage. PhD Thesis. Norwegian University of Science and Technology.

[3] Glatzmaier,G.(2011). *Summary Report for Concentrating Solar Power. Thermal Storage Workshop*. NREL. Retreived 05/11/2013 on http//www.osti.gov/bridge.

[4] Sharma, A., Chen,C.R., Murty,V.V.S & Shukla, A. (2009). Solar Cooker With Latent Heat Storage Systems: A Review. Renewable and Sustainable Energy Reviews 13, 1599-1605. Science Direct. Elsevier

[5] Karaki, W. et. al, (2011). Experimental Investigastion of Thermal Storage Processes in a Thermocline Storage Tank. Proceedings of the ASME 2011. International Conference on Energy Sustainability. Washington DC.USA.

[6] Kuravi, S. et al.(2013). Investigation of a High-Temperature Packed-bed Sensible Heat Thermal Storage System With Large-sized elements. Journal of Solar Energy Engineering, Vol.135/041008-1

Retrieved on 05/11/2013 at: http://Solarenergyengineering.asmedigitalcollection.asme.org.

[7] Tian, Y. & Zhao, C.Y. (2013). A review of Solar Collectors and Thermal Energy Storage in Solar Thermal Applications. Applied Energy. Vol.104, pp.538-553. http://wrap.warwick.ac.uk/52415

[8] Duffie, J & Beckman, W. (1991). Solar Engineering of Thermal Processes. 2nd Edition, John Willey and Sons, Inc. N.Y.

[9] Hanchen, M., Bruckner, S. & Steinfeld, A.(2011). High-temperature Thermal Storage Using a packed bed of Rocks –Heat analysis and Experimental validation. Applied Thermal Engineering 31, 1798-1806. Science Direct. Elsevier.

[10] http://solarcooking.wikia.com/wiki/Solar_Cookers_International_Network_%28Home%29

[11] Lovseth, J.(2011). Isnulation by Evacuation and Multiple Al-foils. In Notes by Jorgen Lovseth. Unpublished.

[12] Bindra, H. et al.(2013). Thermal Analysis and Exergy Evaluation of Packed-bed Thermal Storage Systems. Applied Thermal Engineering, Vol.52, pps 255-263. Science Direct. Elsevier.